Journal Name

RSCPublishing

COMMUNICATION

9,9'-Anthryl-Anthroxyl Radicals: Strategic Stabilization of Highly Reactive Phenoxyl Radicals

Cite this: DOI: 10.1039/xoxxoooooo

Tatsuya Aotake,[a] Mitsuharu Suzuki,[a] Naoki Aratani,[a] Junpei Yuasa,[a] Daiki Kuzuhara,[a] Hironobu Hayashi,[a] Haruyuki Nakano,[b] Tsuyoshi Kawai,[a] Jishan Wu*[c] and Hiroko Yamada*[a,d]

Received ooth January 2012,
Accepted ooth January 2012

DOI: 10.1039/xoxxoooooo

www.rsc.org/

Stable 9,9'-anthryl-anthroxyl radicals were synthesized and isolated, and the structures were fully characterized by single crystal X-ray diffraction analysis and ESR measurement. The resonance structure and steric protection of the peripheral positions and the most reactive 9-position of anthracene prolong the half-life of the radical in solution to 11 days.

Phenoxyl radical,[1] which is one of the highly reactive radicals, is observed in biological processes as tyrosyl radical related to electron transfer, hydrogen atom transfer and proton-coupled electron transfer.[2] It formally contains resonance structure as shown in Scheme 1 and the carbon atom at 4-position is also reactive. The stabilization has been achieved by the bulky ortho-substituents[3], coordination to metal ions[4] or the π-conjugation expansion.[5]

During the synthetic investigation of molecular graphene nano-ribbons (GNRs),[6] we found the formation of stable anthroxyl radical. The preparation of 9,9'-anthryl-anthr-10-oxy radical (**1**), an example of π-expanded phenoxyl radical, was reported by Singer *et al.* in 1971, where **1** was obtained by the oxidation of 9,9'-bianthryl by molecular oxygen, but only the hyperfine coupling constants (hfccs) and *g*-value were reported without an ESR spectrum.[7] Here we will report the synthesis and characterization of stable radical **1**, including the direct comparison of **1** and 10-hydroxy-9,9'-anthyrylanthracene (**1-H**) using the X-ray single crystal structure analysis of co-crystal of **1** and **1-H**. We have also prepared tetrabicyclo-[2.2.2]octadiene(BCOD)-fused 9,9'-anthryl-anthr-10-oxy radical derivative **2** as a more stabilized radical species under ambient conditions. The stability of the compound **2** was attained by two factors: one is the expansion of π-structure: the expansion of phenyl skeleton expanded to anthracene, resulting in the gain of two aromatic stabilization energy as shown in Scheme1, the other is bulky substituents at periphery and at most reactive 9-position. This radical **2** is stable enough to be purified over the conventional silica gel column.

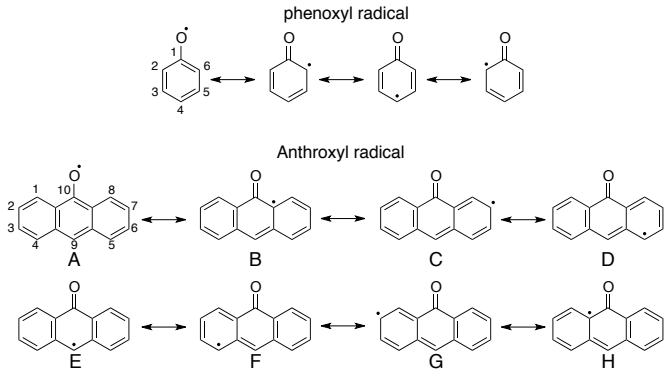

Scheme 1 The resonance structures of phenoxyl radical and anthroxyl radical.

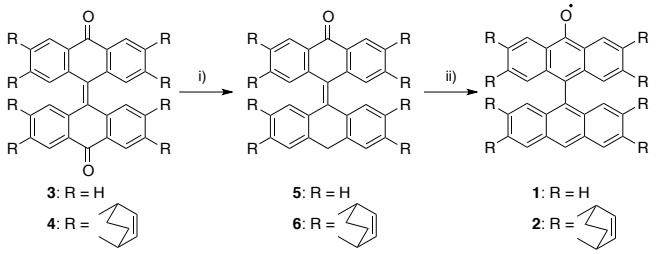

Scheme 2 Syntheses of **1** and **2**: (i) Lithium aluminium hydride (LAH), dry THF, then 6 N HCl, reflux; (ii) $FeSO_4 \cdot 7H_2O$, pyridine-*N*-oxide, pyridine, piperidine, 100 ºC.

Synthetic route of **1** and **2** is shown in Scheme 2. Bisanthracene quinones **3** and **4** were prepared according to the literature.[8,9] Hydride reduction of **3** and **4** using lithium aluminium hydride (LAH) and 6 N HCl produced monoketones **5** and **6**, respectively. The monoketones were used in the following reaction without

purification because of the instability under ambient conditions. The radicals **1** and **2** were obtained by the treatment of monoketones with pyridine *N*-oxide and $FeSO_4 \cdot 7H_2O$ in 15% and 19% yield in 2 steps, respectively. The products were identified by mass spectrum measurement (Fig S1-S3, ESI†), single crystal X-ray diffraction analysis and ESR spectroscopy.

The single crystals were obtained by the diffusion crystallization from chloroform/methanol for **1** and toluene/methanol for **2**. The crystallographic data is summarized in Figs. 1, S4 and S5 and Tables S1–S3, ESI†. The radical **1** gave two types of crystals in one batch: brown needle type and brown plate type. Needle-shaped crystal is the pure crystal of **1**, as shown in Fig 1a and 1b. The crystal data was solved as disordered structure due to the position of oxy-radical unit. The dihedral angle between two-anthracene units is 70.1(2)º. The bond length at C8–C8' is 1.492(3) Å, indicating the single bond. This is different from stable 2,6-di-tert-butyl-4-(4′-nitrophenyl)phenoxyl (^{t}BuNPArO•) radical with the aryl-aryl bond length of 1.4754 Å and the aryl-aryl torsion angle of 17.5º, where the spin density expanded whole molecule.[5b] The crystal with plate-shape contains 10-hydroxy-9,9'-anthyrylanthracene (**1-H**) and the radical **1** as a pair *via* [O-H···O•] hydrogen bonding (Figs. 1c, S4 and S5, ESI†) in co-crystal. The compound **1-H** was obtained from **1** in situ during the crystallizaion. The bond length of O1–C1 of **1-H** is 1.364(3) Å, which confirms to a normal phenoxyl bond. The C–C bond lengths of **1-H** are those of typical aromatic C–C bonds and the bond length of C8–C15 for **1-H** is 1.496(3) Å. Thus **1-H** in the co-crystal is 9,9'-anthryl-10-anthranol. The bond length of O2–C29 of **1** is 1.247(3) Å, which is 0.12 Å shorter than that of O1–C1 of **1-H**. The bond lengths of C29–C42, C29–C30, C35–C36, and C36–C37 are 1.457 (3), 1.464(4), 1.425(3), 1.425(7) Å, assigned to single bonds and the central ring next to the O2 is not aromatic. The bond length of C36–C43 for **1** is 1.492(3) Å. The bond lengths of **1** suggest that a resonant structure E in Scheme 1 mainly contributes to the structure of radical **1**. The radical spin density should be higher at 9-position and the steric protection of the most reactive carbon atom is effective to stabilize the phenoxyl type radicals. The two anthryl units are orthogonal each other with the mutual angles of 87.4(3)º for **1** and 89.1(3)º for **1-H**, respectively. The crystal structure of **2** shows a similar result to the needle-shaped crystal of **1** (Figs. 1d and e). The crystal data was solved as disordered structure due to the position of oxy-radical unit. The two anthracene units are cross-shaped and the dihedral angle is 69.2 (2)º. The C8–C8' bond length that connects two anthracene skeletons is 1.498(3) Å. Co-crystal of **2** and **2-H** was not obtained.

The electronic structures of **1** and **2** were investigated by electron spin resonance (ESR) measurement. The ESR spectra of **1** and **2** in toluene are shown in Fig. 2 together with the simulation pattern. The signals of **1** are attributed to four positions in the anthroxyl skeleton, and the simulated hfccs are 0.90 (2H), 3.28 (2H), 0.90 (2H) and 3.28 G (2H). The *g*-value is 2.0023, which corresponds to a general organic free radical compound. The line width of the ESR spectrum of **2** was wider than **1** and the spectrum was hardly changed even by varying the temperature. The signals of **2** are ascribed to the two positions in the skeleton. The simulated hfccs are 1.00 (2H), 2.80 G (2H) and the *g*-value is 2.0024. According to the spin density calculation (Figs. 2c,d), both **1** and **2** have the highest spin densities on the C8 substituted with anthryl or its derivative (For numbering, see Fig. 1). This result suggests the resonant structure E in Scheme 1 is also the main structure for **1** and **2** in solution. The anthryl groups are substantially orthogonal to phenoxyl skeleton, contributing as steric protection to the radical. Density functional theory (DFT) calculations at the B3LYP/6-31G(d) level were conducted to provide a further understanding of SOMO.[10] Computed spin densities showed that the unpaired electrons were delocalized on anthroxyl

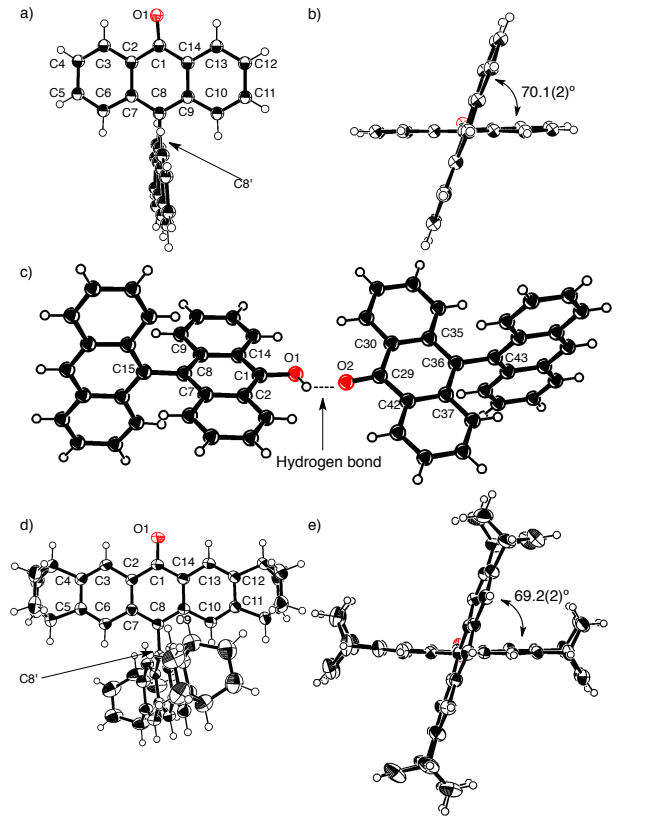

Fig. 1 Crystal structures of a) top view; and b) side view of **1**; c) co-crystal with **1** and anthroxyl anthracene (**1-H**); d) top view; and e) side view of **2**. Solvent molecules are omitted for clarity. Thermal ellipsoids represent 50% probability.

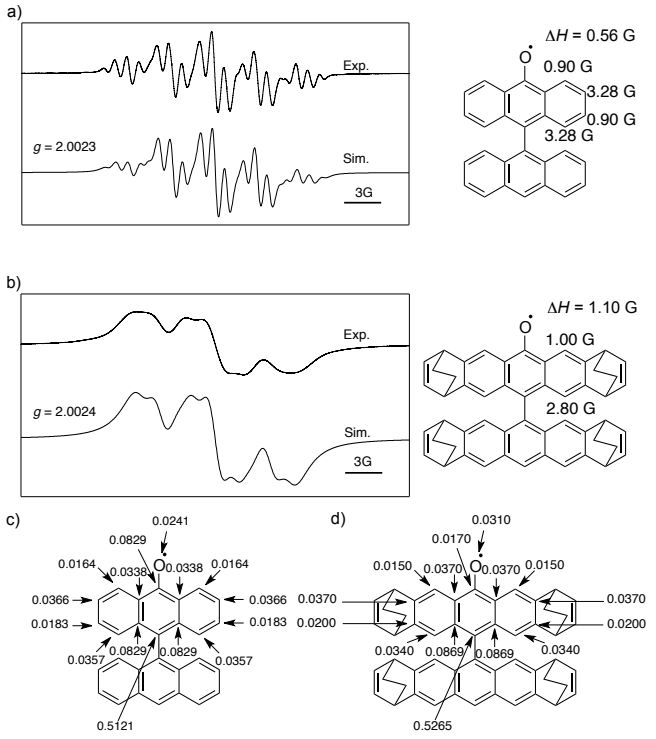

Fig. 2 ESR spectra and simulation of a) **1** in toluene (1.6×10^{-2} mM) at 183 K and b) **2** in toluene (2.7×10^{-2} mM) at 183 K. Spin density of c) **1**; and d) **2** computed at the B3LYP/6-31G(d) level.

skeleton for each compound rather than the subsituent-acenes (Fig. S6, ESI†).

The UV-vis absorption spectra of **1** and **2** recorded in toluene are shown in Fig. 3a and Table 1. Each solution displayed a dark yellow color. The UV-vis absorption spectrum of **1** shows the major absorption at 357 (ε = 23,900 $M^{-1}cm^{-1}$) and 387 nm (ε = 12,900 $M^{-1}cm^{-1}$) and the minor absorption broadened to 800 nm with maxima at 413 (ε = 5,590 $M^{-1}cm^{-1}$), 434 (ε = 6,660 $M^{-1}cm^{-1}$), 537 (ε = 1,620 $M^{-1}cm^{-1}$) and 578 nm (ε = 1,830 $M^{-1}cm^{-1}$). Since the UV-vis absorption spectrum of 9,9'-bianthryl is up to 400 nm,[11] the absorption wavelength is red-shifted by the contribution of SOMO, as shown by the TD-DFT calculations (Fig. S7, ESI†). The BCOD-fused compound **2** displays an absorption spectrum with the red-shifted major absorption at 369 (ε = 25,000 $M^{-1}cm^{-1}$) and 384 (ε = 12,800 $M^{-1}cm^{-1}$) nm, and with the minor absorption broader and spread to 800 nm compared to **1**. The photo-stability of the radical in toluene was checked by UV-vis absorption spectral change. The solution was kept under room light under air and the temporal spectral change was measured, as shown in Figs. 3b, S8 and S9, ESI†. The peak-top (357 nm) of the absorbance of **1** is gradually decreased and the half life ($\tau_{1/2}$) is calculated to be 92 h. In contrast, $\tau_{1/2}$ of **2** was significantly longer than **1** and was estimated as 274 h (11.4 d). The stability was improved about 3 times by inserting the BCOD moieties.

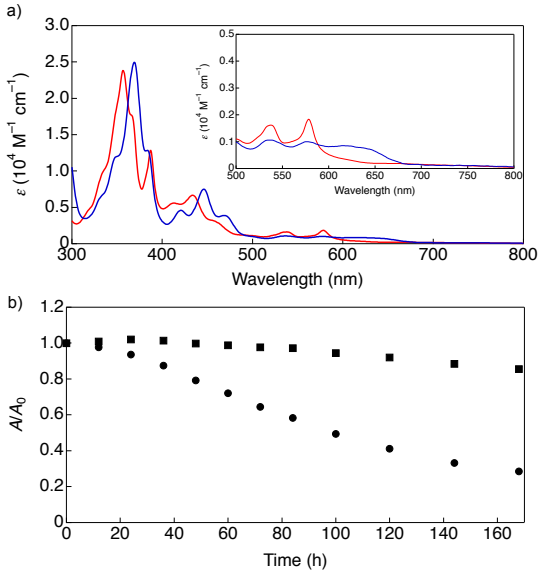

Fig. 3 a) UV-Vis absorption spectra of **1** (red line) and **2** (blue line) in toluene. b) Decay profiles of UV-vis absorption spectra a) **1** (●357 nm) and b) **2** (■369 nm).

Table 1 Summary of optical and electrochemical properties of radicals.

Compd.	λ_{abs} (nm)[a]	E_{ox}(V)[b]	E_{red} (V)[b]
1	357, 387, 413, 434, 537, 578	0.55	–0.77
2	369, 384, 421, 446, 537, 576, 615	0.25, 0.91	–0.94

[a]In toluene. [b]The values were obtained by cyclic voltammetry. V vs. Fc/Fc^+.

The electrochemical properties of the radicals were studied by cyclic voltammetry (CV) in dry dichloromethane containing 0.1 M tetra-*n*-buthylammonium hexafluorophosphate ($n$$Bu_4NPF_6$) as a supporting electrolyte. The results are summarized in Table 1 and Fig. S10, ESI†. The one-electron reduction potentials ($E_{red}^{1/2}$ *vs.* Fc/Fc^+) of **1** and **2** are at –0.77 V and –0.94 V, respectively. The radical **1** shows one oxidation potential at 0.55 V (*vs.* Fc/Fc^+), whereas **2** shows two reversible oxidation waves at 0.25 and 0.91 V (*vs.* Fc/Fc^+). In comparison with **1**, the first oxidation and reduction potentials of compound **2** are shifted to negative side. It is considered that the SOMO energy level of **2** rises by receiving the electric effect of σ-π hyperconjugation of BCOD-units to anthracene moiety.[12] From CV and DFT calculations, stability of **2** against electrochemical oxidation is predicted to be lower than that of **1**. The surrounding structures of C8 position of **1** and **2** are similar in crystals due to the similarity of the angles of two anthryl planes and the C8-C8' distances. However, the better stability of **2** in solution suggests the restricted rotation freedom on C8-C8' axis for **2** compared to **1** owing the BCOD substituents at the edge of anthracene unit, thus restrict the reactivity of C8 to give quinoid structure (Fig. S11, ESI†).

In conclusion, we were successful to prepare and characterize the stable 9,9'-anthryl-anthroxylradicals. The result of X-ray structural analysis, ESR spectra and DFT calculations suggested the highest spin density of radical **1** localized at 9-position due to the resonance and the stabilization of the phenoxyl radical achieved by protection of the most reactive position with an anthryl group. The peripheral BCOD-substituents influenced the energy levels of SOMOs to be raised by σ-π hyperconjugation to encourage the electrochemical oxidation and the absorption spectrum to be red-shifted. Furthermore the stability of the radical **2** in solution was improved owing to the steric hindrance of BCOD-moiety to restrict the rotation around the C8-C8' axis. Finally we have tried to prepare 6,6'-penthryl-penthroxy radical (**7**) from **2** by retro-Diels–Alder reaction.[8,13] Although the formation of pentacene dimer was detected[14] the ESR measurement of the product was not successful at the present because the life-time of the product is much shorter than that of **1**.

The authors thank Ms. Yoshiko Nishikawa in NAIST for the measurement of mass spectra, Mr. Fumio Asanoma in NAIST for the measurement of ESR spectra, Mr. Shouhei Katao in NAIST for the measurement of single-crystal structure analysis. This work was partly supported by Grants-in Aid (No. 22350083 and 26105004 to H.Y. and No. 26288038 to N.A.), the Green Photonics Project in NAIST and the program for promoting the enhancement of research universities in NAIST supported by MEXT. J.W. acknowledges financial support from Singapore MOE Tier 2 grant (MOE2014-T2-1-080).

Notes and references

[a] Graduate School of Materials Science, Nara Institute of Science and Technology (NAIST), 8916-5 Takayama-cho, Ikoma 630-0192 (Japan)
[b] Department of Chemistry Graduate School of Sciences, Kyushu University, Fukuoka 812-8581 (Japan)
[c] National University of Singapore3 Science Drive 3, 117543 (Singapore)
[d] CREST, Japan Science and Technology Agency (JST) 4-1-8 Honcho, Kawaguchi, Saitama 332-0012 (Japan)

† CCDC numbers of crystal of **1**, co-crystal of **1** and **1-H**, and crystal of **2** are 1021762, 1021763, and 1021764, respectively. Electronic Supplementary Information (ESI) available: [synthetic details, X-ray crystal structural analysis, DFT calculations, time profiles of UV-vis absorption spectra, and thermal analysis]. See DOI: 10.1039/c000000x/

1 R. Pummerer and F. Frankfurter, *Chem. Ber.,* 1914, **47**, 1472.
2 (*a*) R. W. Kreilick and S. I. Weissman, *J. Am. Chem. Soc.*, 1962, **84**, 306; (*b*) H.-J. Krüger, *Angew. Chem. Int. Ed.,* 1999, **38**, 627; (*c*) S. Itoh, M. Taki and S. Fukuzumi, *Coord. Chem. Rev.,* 2000, **198**, 3; (*d*) C. T. Lyons and T. D. P. Stack, *Coord. Chem. Rev.,* 2013, **257**, 528.

3 (*a*) E. Müller, A. Schick and K. Scheffler, *Chem. Ber.*, 1959, **92**, 474; (*b*) E. R. Altwicker, *Chem. Rev.,* 1967, **67**, 475; (*c*) V. W. Manner, T. F. Markle, J. H. Freudenthal, S. P. Roth and J. M. Mayer, *Chem. Commun*., 2008, 256. (*d*) J. M. Wittman, R. Hayoun, W. Kaminsky, M. K. Coggins and J. Mayer, *J. Am. Chem. Soc*., 2013, **135**, 12956.

4 (*a*) A. Sokolowski, J. Müller, T. Weyhermüller, R. Schnepf, P. Hildebrandt, K. Hildenbrand, E. Bothe and K. Wieghardt, *J. Am. Chem. Soc*., 1997, **119**, 8889; (*b*) A. Philibert, F. Thomas, C. Philouze, S. Hamman, E. Saint-Aman and J.-L, Pierre, *Chem. Eur. J.,* 2003, **9**, 3803; *(c*) Y. Shimazaki, S. Huth, S. Karasawa, S. Hirota, Y. Naruta, O. Yamaguchi, *Inorg. Chem*., 2004, **43**, 7816.

5 (*a*) C. Xie, P. M. Lahti and C. George, *Org. Lett.*, 2000, **2**, 3417; (*b*) T. R. Porter, W. Kaminsky and J. M. Mayer, *J. Org. Chem.,* 2014, **79**, 9451.

6 (*a*) J. Cai, P. Ruffieux, R. Jaafar, M. Bieri, T. Braun, S. Blankenburg, M. Muoth, A. P. Seitsonen, M. Saleh, X. Feng, K. Müllen and R. Fasel, *Nature,* 2010, **466**, 470; (*b*) L. Chen, Y. Hernandez, X. Feng and K. Müllen, *Angew. Chem. Int. Ed*., 2012, **51**, 7640; (*c*) A. Konishi, Y. Hirao, K. Matsumoto, H. Kurata, R. Kishi, Y. Shigeta, M. Nakano, K. Tokunaga, K. Kamada and T. Kubo, *J. Am Chem. Soc.,* 2013, **135**, 1430.

7 L. S. Singer, I. C. Lewis, T. Richerzhagen and G. Vincow, *J. Phys. Chem.,* 1971, **75**, 290.

8 K. Tanaka, N. Aratani, D. Kuzuhara, S. Sakamoto, T. Okujima, N. Ono, H. Uno and H. Yamada, *RSC Adv.,* 2013, **3**, 15310.

9 (*a*) S. M. Arabei and T. A. Pavich, *J. Appl. Spectrosc.,* 2000, **67**, 236; (*b*) X. Zhang, J. Li, H. Qu, C. Chi and J. Wu, *Org. Lett.*, 2010, **12**, 3964.

10 Gaussian 09, Revision D.01, M. J. Frisch, et al. See the ESI for details.

11 P. Natarajan and M. Schmittle, *J. Org. Chem.,* 2013, **78**, 10383.

12 (*a*) K. Komatsu, H. Akamatsu, Y. Jinbu and K. Okamoto, *J. Am. Chem. Soc.,* 1988, **110**, 633; (*b*) A. Matsuura, T. Nishinaga and K. Komatsu, *J. Am. Chem. Soc.,* 2000, **122**, 10007.

13 (*a*) S. Ito, T. Murashima, N. Ono and H. Uno, *Chem. Commun.,* 1998, 1661; (*b*) H. Yamada, T. Okujima and N. Ono, *Chem. Commun.,* 2008, 2957.

14 The weight loss in thermogravimetric analysis of **2** (Fig. S12, ESI†) starts at 200 ºC and ends around 300 ºC, but soon the weight loss started again. The preparation of radical **7** was tried by heating by microwave in ethyleneglycol at 300 ºC for 5 min under argon atmosphere. After the quick filtration, the precipitate was suggested to have pentacene dimer unit by APCI-Mass measurement (Fig. S13, ESI†).

